A Mutation in Subunit I of Cytochrome Oxidase from *Rhodobacter sphaeroides* Results in an Increase in Steady-State Activity but Completely Eliminates Proton Pumping†

Ashtamurthy S. Pawate,‡ Joel Morgan,§ Andreas Namslauer,|| Denise Mills,⊥ Peter Brzezinski,|| Shelagh Ferguson-Miller,⊥ and Robert B. Gennis*,‡,§

Center for Biophysics and Computational Biology and Department of Biochemistry, University of Illinois, Urbana, Illinois 61801, Department of Biochemistry and Biophysics, The Arrhenius Laboratories for Natural Sciences, Stockholm University, SE-106 91 Stockholm, Sweden, and Department of Biochemistry, Michigan State University, East Lansing, Michigan 48824

Received August 6, 2002; Revised Manuscript Received September 7, 2002

ABSTRACT: The heme−copper oxidases convert the free energy liberated in the reduction of O_2 to water into a transmembrane proton electrochemical potential (protonmotive force). One of the essential structural elements of the enzyme is the D-channel, which is thought to be the input pathway, both for protons which go to form H_2O ("chemical protons") and for protons that get translocated across the lipid membrane ("pumped protons"). The D-channel contains a chain of water molecules extending about 25 Å from an aspartic acid (D132 in the *Rhodobacter sphaeroides* oxidase) near the cytoplasmic ("inside") enzyme surface to a glutamic acid (E286) in the protein interior. Mutations in which either of these acidic residues is replaced by their corresponding amides (D132N or E286Q) result in severe inhibition of enzyme activity. In the current work, an asparagine located in the D-channel has been replaced by the corresponding acid (N139 to D; N98 in bovine enzyme) with dramatic consequences. The N139D mutation not only completely eliminates proton pumping but, at the same time, confers a substantial increase (150−300%) in the steady-state cytochrome oxidase activity. The N139D mutant of the *R. sphaeroides* oxidase was further characterized by examining the rates of individual steps in the catalytic cycle. Under anaerobic conditions, the rate of reduction of heme a_3 in the fully oxidized enzyme, prior to the reaction with O_2, is identical to that of the wild-type oxidase and is not accelerated. However, the rate of reaction of the fully reduced enzyme with O_2 is accelerated by the N139D mutation, as shown by a more rapid **F** → **O** transition. Whereas the rates of formation and decay of the oxygenated intermediates are altered, the nature of the oxygenated intermediates is not perturbed by the N139D mutation.

The heme−copper oxidases are the terminal enzymes in the aerobic respiratory chains of most eukaryotes and prokaryotes (*1*). These enzymes comprise a superfamily which utilizes different substrates (quinones, cytochrome *c*'s, or HiPip Fe-S proteins) and includes members with different heme components (hemes A, B, O, or C) (*1*−*4*). These enzymes reduce O_2 to water at a heme−copper binuclear center, and all possess a low-spin heme which routes electrons to the active site. The cytochrome *c* oxidases have a dinuclear copper center (Cu_A) which passes electrons to the low-spin heme. In the cytochrome *c* oxidase from *Rhodobacter sphaeroides* both hemes are A. The heme−copper oxidases are all proton pumps, and it is this aspect which has motivated much of the research interest in these enzymes. The X-ray structures of several heme−copper oxidases have been determined (*5*−*13*). Although these structures have propelled research forward, the fundamental questions about how the proton pump works and how it is coupled to the reduction of O_2 to H_2O remain a mystery (*14*−*18*). In the current work, a mutation is described which decouples the proton pump from the redox chemistry and also increases the steady-state turnover of the *R. sphaeroides* aa_3-type oxidase. This mutation, which is located within the D-channel (see below), may provide insight into the mechanism of the proton pump.

Site-directed mutagenesis has been of central importance to define the two proton translocation pathways within the bacterial enzymes: the K-channel and the D-channel (*14*, *19*−*25*). The K-channel, so-called because of a critical lysine residue (K362)[1] in its center, begins at a glutamic acid residue in subunit II ($E101^{II}$) on the cytoplasmic surface of the enzyme and terminates at a tyrosine (Y288) at the heme−copper oxygen reduction site. The tyrosine is cross-linked to H284 (*6*, *12*, *26*, *27*), a ligand to Cu_B, and is directly

† Supported by grants from the National Institutes of Health [HL16101 (R.B.G.) and GM26916 (S.F.-M.)], the Human Frontier Science Program [RG0135 (R.B.G., P.B., and S.F.-M.)], The Swedish Foundation for International Cooperation in Research and Higher Education (P.B.), and the Swedish Research Council (P.B.).

* Corresponding author: telephone, 217-333-9075; fax, 217-244-3186; e-mail, r-gennis@uiuc.edu.

‡ Center for Biophysics and Computational Biology, University of Illinois.

§ Department of Biochemistry, University of Illinois.

|| Stockholm University.

⊥ Michigan State University.

[1] *R. sphaeroides* numbering is used throughout.

10.1021/bi026582+ CCC: $22.00
Published on Web 10/11/2002

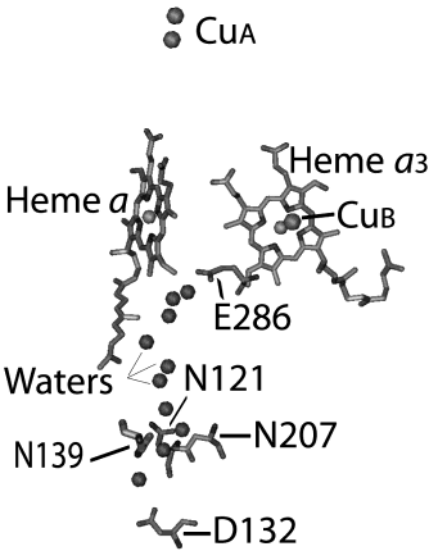

FIGURE 1: Structure of the D-channel showing the location of the channel entrance at D132, the cluster of asparagines N121, N139, and N207, and the last residue E286. The waters in the channel are shown as spheres. The distances (Cα−Cα) are 10.7 Å for D132−N139 and 20.6 Å for N139−E286. The structure coordinates were from So Iwata (personal communication). The software used for visualization was VMD (*54*).

involved in the catalysis of O−O bond breaking (*22*, *28*, *29*). Mutations within the K-channel result in greatly reduced steady-state cytochrome *c* oxidase activity. The K362M mutant is virtually inactive (<0.05% turnover). Those mutants with residual activity (e.g., T352A, T359A) pump protons with the same stoichiometry as does the wild-type enzyme (1 H^+/e^-) (*30*). The low rate of turnover of the K-channel mutants is due to selective inhibition of reduction of the heme−copper center prior to the reaction with O_2 (*31*, *32*). Reduction of heme a_3 requires the concomitant transfer of a proton to the enzyme active site via the K-channel, presumably converting an $^-$OH bound to the heme a_3 iron to H_2O. No data implicate the K-channel in a direct role in proton pumping, though this possibility cannot be excluded.

The D-channel is defined by an aspartic acid (D132) near the protein surface (bacterial cytoplasm) and a glutamic acid (E286) about 25 Å away from D132 and 12 Å from the heme−copper center. Between these two acidic residues is a chain of water molecules that presumably provides a pathway to facilitate proton transfer (Figure 1). The D132N and D132A mutations in the *R. sphaeroides* oxidase result in <5% turnover and eliminate proton pumping (*33*). It appears that the D132 mutations completely block proton uptake into the D-channel but that there is residual activity due to protons leaking from the periplasmic side of the enzyme, possibly through the exit channel usually used by pumped protons (*30*, *33*−*35*). These "leaked" protons are consumed at the active site to generate water (*30*, *33*, *34*).

Replacement of E286 (E286Q,A) virtually eliminates turnover (<0.5%) in the *R. sphaeroides* oxidase (*23*, *35*). This block can be partially reversed by placing a glutamic acid side chain on another transmembrane helix but in the same spatial position. For example, the double mutant E286A/I112E has higher turnover activity than the E286A single mutant (approximately 5% that of the wild-type enzyme) and pumps protons (*36*). Similarly, the nearly complete block due to the equivalent mutation in the *P. denitrificans* oxidase is partially reversed (10% turnover accompanied by proton pumping) by a mutation that places a tyrosine at the same spatial position, mimicking sequences found in several other oxidases (*37*).

These data indicate that proton pumping requires a supply of protons coming through the D-channel from D132 to E286 or to a suitable substitute residue providing a protonatable group with a high p*K* (about 10) at the same spatial location as E286. The data also implicate the D-channel in supplying at least some, if not all, of the protons for the reduction of O_2 to H_2O, since blocking the entrance of the D-channel (D132N) drastically diminishes oxidase activity. The residual activity (<5% of wild type) is due to leak of protons to the active site, mainly from the outer (periplasmic) side of the membrane. The pathways for proton transfer beyond E286 are not known, nor is the nature of the "switch" that directs protons from the D-channel to either the active site (chemical protons) or to the exit channel (pumped protons) (*38*). The chemical basis for the predominately unidirectional flux of pumped protons (i.e., the gating switch) is also not known.

The current work was motivated by the report of a mutation within the D-channel of the oxidase from *Paracoccus denitrificans* which resulted in an "ideal decoupled" phenotype, i.e., 100% oxidase activity but no proton pumping (*25*). The mutation replaces an asparagine (N131; *P. denitrificans* numbering) in the D-channel by an aspartic acid. The corresponding mutation in the *E. coli* cytochrome bo_3 quinol oxidase (N142D; *E. coli* numbering) was reported previously to have about 50% of the oxidase activity and to pump protons (*39*).

Because of the experimental value of having a mutant that selectively disables the proton pump without diminishing the oxidase activity, the corresponding mutation (N139D) was made in the *R. sphaeroides* oxidase. This residue is located near D132 (<10 Å) and is 20 Å from E286 (Figure 1). Remarkably, the resulting N139D mutant has a substantially higher turnover rate than does the wild-type enzyme (150−300%, in different preparations), but proton pumping is completely eliminated. The ideal decoupled phenotype (*25*) is, thus, confirmed. Several of the individual steps in the reaction sequence were examined in isolation by single-turnover techniques. The rate of reduction of the fully oxidized enzyme, specifically reduction of heme a_3 by heme *a*, is not altered by the N139D mutation. The flow-flash technique was used to determine the rate of reaction of the fully reduced enzyme with O_2. The N139D mutant exhibited an increased (2-fold) rate for the **F** → **O** transition, consistent with the increased rate of steady-state turnover. The UV−vis spectra of the reaction intermediates ($\mathbf{P_R}$ and **F**) are not altered by the mutation, showing that the mutation does not alter the reaction mechanism for the oxygen chemistry at the active site. Possible mechanisms for how this single mutation might disable the proton pump while accelerating turnover are discussed.

MATERIALS AND METHODS

Materials. Dodecyl β-D-maltoside (DM)[2] and sodium cholate were obtained from Anatrace. Ni^{2+}-NTA agarose was

[2] Abbreviations: COV, cytochrome oxidase vesicles; FCCP, carbonyl cyanide *p*-(trifluoromethyloxy)phenylhydrazone; WT, wild-type enzyme; TMPD, *N*,*N*,*N*′,*N*′-tetramethylphenylenediamine; DM, dodecyl β-D-maltoside.

obtained from Qiagen. CCCP, valinomycin, ferricyanide, dithionite, and horse heart cytochrome *c* were from Sigma. DNA oligonucleotides were synthesized by the University of Illinois Biotechnology Center (Urbana, IL). QuikChange site-directed mutagenesis kits were obtained from Stratagene. Restriction enzymes were obtained from New England Biolabs and Gibco-BRL.

Site-Directed Mutagenesis. The N139D mutation in subunit I was created with the QuikChange site-directed mutagenesis kit (Stratagene). The gene was partially sequenced to verify the mutation and to check for any mistakes that might have occurred elsewhere.

Protein Preparation. Histidine-tagged wild-type and mutant cytochrome *c* oxidases were purified from *R. sphaeroides*, and the concentration was determined by UV−vis spectroscopy as described previously (*40*). Further purification was done by fast protein liquid chromatography (Amersham Biosciences, Inc., AKTA-519) with tandem DEAE-5PW columns (Toso-Haas) (*44*).

Steady-State Kinetics. Steady-state activity was measured polarographically using a YSI model 53 oxygen meter. A 1.8 mL amount of 50 mM phosphate buffer, pH 7.4, containing 0.1% DM and 1.1 mg/mL asolectin and supplemented with 2.8 mM ascorbate and 0.55 mM TMPD was placed in the sample chamber. Cytochrome *c* was added to a final concentration of 40 μM. The reaction was initiated by adding 1, 2, 4, and 8 μL of 1 μM enzyme, and oxygen consumption was monitored.

For experiments with reconstituted cytochrome oxidase vesicles, the potassium ionophore valinomycin and the uncoupler FCCP were added sequentially after the addition of the COVs to the assay buffer (5.7 mM ascorbate, 0.28 mM TMPD, 24 mM KCl, and 50 mM HEPES−KOH, pH 7.4).

The enzyme activity in electrons consumed per second per enzyme complex was calculated from the oxygen consumption traces.

Flow-Flash Kinetics. The flow-flash method was used to study the reaction between fully reduced cytochrome *c* oxidase and oxygen. The experimental setup is described in detail in ref *20*.

The enzyme solution was diluted to a concentration of ~10 μM in 100 mM HEPES, pH 7.4, and 0.1% DM and transferred to an anaerobic cuvette. Phenazine methosulfate was added to a final concentration of 1 μM, and air in the cuvette was exchanged for N_2 on a vacuum/gas line. The sample was reduced by addition of 2 mM ascorbate, and formation of the fully reduced state after ~1 h of incubation was confirmed by the optical absorption spectrum of the sample. N_2 was replaced by CO, and the binding of CO to the enzyme was verified spectroscopically.

The sample was transferred anaerobically to one of the drive syringes (0.5 mL) of a custom-built stopped-flow/flash-photolysis apparatus (Applied Photophysics, Surrey, U.K.). The other drive (2.5 mL) syringe was filled with oxygen-saturated buffer, 100 mM HEPES, pH 7.4, and 0.1% dodecyl β-D-maltoside. The reaction was initiated by photodissociation of the bound CO with a 5 ns laser flash at 532 nm, which was fired ~100 ms after mixing. Absorbance changes were recorded at single wavelengths as a function of time. The rate constants and amplitudes of the transient absorbance changes during the reaction were analyzed by fitting the data to a multiexponential function using the ProK software (Applied Photophysics, Surrey, U.K.).

Low-Temperature Kinetics. Low-temperature flow-flash measurements were done as described previously (*41*). In brief, the enzyme was made anaerobic by argon exchange on a gas/vacuum line, reduced by adding 1 mM ascorbate and 0.1 mM TMPD, and mixed with CO. The CO-bound reduced enzyme was mixed with the cryoprotectant ethylene glycol to a final concentration of 50% ethylene glycol, and the cuvette was placed in a cuvette holder which was then cooled to −24 °C using a Neslab RTE-140 thermostat. The cuvette was kept dry by a continuous flow of nitrogen gas in the cuvette holder. Oxygen-saturated buffer with 50% ethylene glycol at −24 °C was mixed with the sample in a 1:1 ratio. The reaction was initiated by a camera flash, and data were collected on an Applied Photophysics diode array spectrophotometer attached by fiber optic or liquid light guides to the cuvette holder. Data points were collected every 2.5 ms with a wavelength pitch of 3.4 nm. An electrically driven shutter (Uniblitz VMM-T1/VS25; Vincent Associates, Rochester, NY) was used to keep the sample in the dark during O_2 addition. The shutter was opened a few milliseconds prior to the start of the reaction.

Rereduction Kinetics. Rereduction kinetics were studied in an Applied Photophysics stopped-flow spectrophotometer equipped with a diode array detector, using ruthenium(II) hexaamine as electron donor (*42*). Oxidase (8 μM) was added to 200 mM Tricine, pH 8.0, and 0.1% dodecyl maltoside, and the mixture was placed in a reservoir made from a syringe barrel at the loading position of the stopped-flow unit. The solution was made oxygen free by directing a gentle jet of argon or nitrogen gas over the solution. Ruthenium(III) hexaamine (10 mM) was added together with 60 mM dithionite to reduce the enzyme, and the sample was then loaded into one of the driving syringes. Air-saturated buffer containing 0.1% DM was placed in the second driving syringe. Upon mixing, the oxidation of the enzyme and reduction of heme *a* are both essentially complete within the dead time of the instrument. The excess dithionite rapidly removes any oxygen remaining in the solution. This makes it possible to measure the reduction of heme a_3.

Reconstitution of Oxidase in Proteoliposomes. Cytochrome oxidase vesicles (COVs) were made by the cholate dialysis method (*43*). Purified asolectin was suspended at 40 mg mL^{-1} in 2% cholate and 75 mM HEPES−KOH, pH 7.4, and sonicated until the solution was clear. Cytochrome oxidase was incubated on ice at 4 μM final concentration in 75 mM HEPES−KOH, pH 7.4, and 4% cholate for 1 h. This was mixed with the sonicated asolectin to a final concentration of 2 μM oxidase and 20 mg mL^{-1} lipid. COV formation was by dialysis, using progressively weaker buffers, in the following manner: buffer A (75 mM HEPES−KOH, pH 7.4, 14 mM KCl, 0.1% cholate); buffer B (75 mM HEPES−KOH, pH 7.4, 14 mM KCl); buffer C (50 mM HEPES−KOH, pH 7.4, 25 mM KCl, 15 mM sucrose); buffers D and E (50 μM HEPES−KOH, pH 7.4, 45 mM KCl). The volume of the COV suspension was measured and the concentration of the protein determined by comparing the volumes before and after dialysis.

Proton Pumping Measurements. Proton pumping of the COVs was measured by observing the absorbance changes in the pH-sensitive dye phenol red in a rapid scanning

Table 1: Cytochrome *c* Oxidase Activity of the Wild-Type and N139D Mutant Enzymes

method	enzyme state	WT activity (e^-/s per aa_3)	N139D activity (e^-/s per aa_3)
O_2 consumption	solubilized[a]	1240	3340
	COV (controlled)[b]	41	106
	COV (uncontrolled)[c]	379	724
cytochrome *c* oxidation	COV (controlled)[b]	31	165
	COV (uncontrolled)[c]	387	999

[a] Purified enzyme solubilized in dodecyl maltoside. [b] Controlled activity refers to measurements of the enzyme activity in reconstituted vesicles in the absence of uncoupler (FCCP) and ionophore (valinomycin). [c] Uncontrolled activity refers to measurements of the enzyme activity in reconstituted vesicles in the presence of FCCP and valinomycin.

stopped-flow spectrophotometer (Olis RSM). Horse heart cytochrome *c* was prereduced with dithionite, desalted through a Sephadex G-75 column in 0.5 mM HEPES−KOH, pH 7.4, 45 mM KCl, and 1 mM EDTA, and then concentrated to about 1 mM. Stopped-flow measurements were done in 50 μM HEPES−KOH, pH 7.4, 45 mM KCl, and 100 μM phenol red. Kinetics of cytochrome *c* oxidation were determined by a single-exponential global fit using the Olis RSM-1000 software. Absorbance changes due to phenol red were followed at 557 nm, the isosbestic point for reduced and oxidized cytochrome *c*. Several data sets were collected, and data were analyzed using procedures previously described (*44*).

Data Analysis. Data analysis for the low-temperature flow-flash kinetics and rereduction kinetics was done using MATLAB (The Mathworks, South Natick, MA) DISCRETE and SPLMOD (*45*) implementation as in Morgan et al. (*46*).

RESULTS

Both the wild-type and N139D mutant oxidases were isolated using a histidine tag on the C-terminus of subunit I. The UV−vis spectroscopic features of the mutant oxidase are indistinguishable from those of the wild type (not shown). Several different preparations of the enzyme were used to compare activities. The results for one preparation are shown in Table 1. The cytochrome *c* oxidase turnover number of the N139D mutant of this preparation was 3340 e^-/s, compared to 1240 e^-/s for the wild-type control. The turnover rate of the mutant was preparation dependent and ranged from ~1.5- to 3-fold of the wild-type control assayed under the same conditions.

The oxidase was reconstituted into phospholipid vesicles using procedures to yield COVs (cytochrome oxidase vesicles) suitable for measuring proton pumping. The cytochrome *c* oxidase activity of the COVs was measured polarographically, monitoring oxygen consumption using an oxygen electrode (Table 1; O_2 consumption), and spectroscopically, by monitoring the oxidation of cytochrome *c* (Table 1; cytochrome *c* oxidation). Note that the activity values in Table 1 for the COVs are not measured under saturating condition, or near V_{max}, but under conditions similar to those used for the proton pumping experiments (see below). The measurements were performed (1) in the presence of valinomycin plus FCCP (denoted "uncontrolled"), which allow equilibration of both K^+ and H^+ across

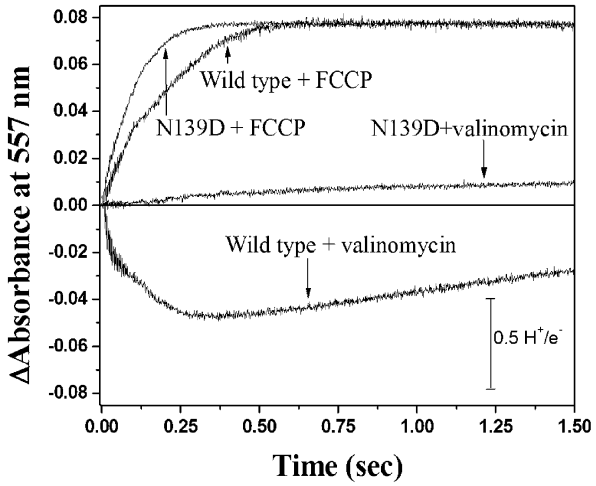

FIGURE 2: Phenol red absorbance followed at 557 nm showing that the wild-type enzyme pumps protons but not the mutant enzyme. COVs prepared by the dialysis method were mixed with reduced cytochrome *c* (enough for 20 or 40 turnovers) and 100 μM phenol red in an Olis stopped-flow spectrophotometer. Acidification of phenol red due to proton pumping is detected as a decrease in absorbance. The uncoupled enzyme shows only alkalinization, as indicated by the increase in absorbance of phenol red. The amplitude of this absorbance change is used for calibration, assuming that the buffering capacity before and after addition of the uncoupler remains constant.

the vesicle membrane, preventing a protonmotive force from developing, and (2) in the absence of the ionophores (denoted "controlled"), in which case a protonmotive force is generated. The enzyme velocity measured under identical conditions is consistently higher for the N139D mutant than for the wild-type oxidase. The N139D mutant exhibits about a 5-fold increase in activity in the presence of uncouplers, compared to about a 10-fold increase for the wild-type oxidase. The persistence of respiratory control shows that the mutant oxidase vesicles are intact and can maintain a transmembrane potential. Importantly, the data also demonstrate that the turnover of the N139D oxidase involves one or more rate-determining steps that require the net outward electrogenic transfer of positive charge (or negative charge inward) across the vesicle membrane. The magnitude of control of the enzyme turnover rate by the opposing protonmotive force that develops across the membrane is less than in the case of the wild-type oxidase, but is still substantial. Charge separation by the wild-type oxidase proceeds by two mechanisms: (1) separation of the source of protons and electrons from opposite sides of the membrane to form water when combined with O_2 at the heme−copper center and (2) proton pumping. As shown below, proton pumping is absent in the N139D mutant. The fact that the enzyme still exhibits respiratory control shows that a membrane potential is developed due to the consumption of protons on the inside of the vesicles. Thus, the mutation does not simply create a rapid leakage pathway for protons across the membrane, in which case no respiratory control would be present.

Figure 2 shows proton pumping assays on the N139D mutant and wild-type oxidase measured on the purified enzymes reconstituted in the phospholipid vesicles. The reaction was carried out by mixing reduced cytochrome *c* with COVs in the presence of air in a stopped-flow spectrophotometer, and the consumption of the chemical

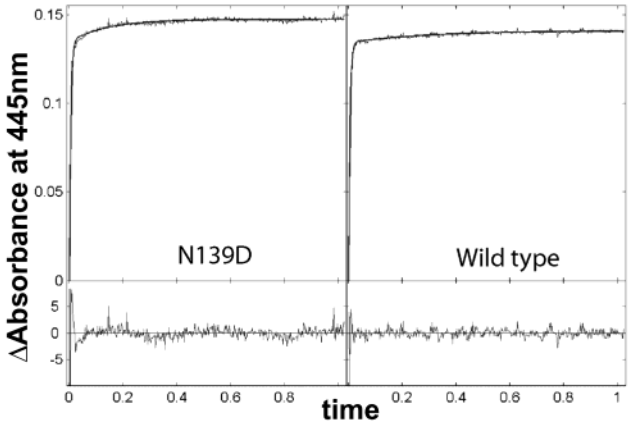

FIGURE 3: Rereduction kinetics. The time course of the absorbance changes at 445 nm was fit to multiexponential kinetic models using DISCRETE. The surface of absorbance changes was corrected for baseline jitter by subtraction of the average of a set of absorbance traces between 680 and 700 nm from the same surface before fitting the data. The mutant enzyme (left) and the wild-type enzyme (right) show similar rates for reduction. Both traces yield two-exponential fits: a fast phase with a large amplitude (~90%) and a slow phase with a smaller amplitude (~10%). The fast phase rate constants were 196 s^{-1} and 194 s^{-1} for the mutant and wild-type enzyme, respectively. Residuals are shown in the lower panels.

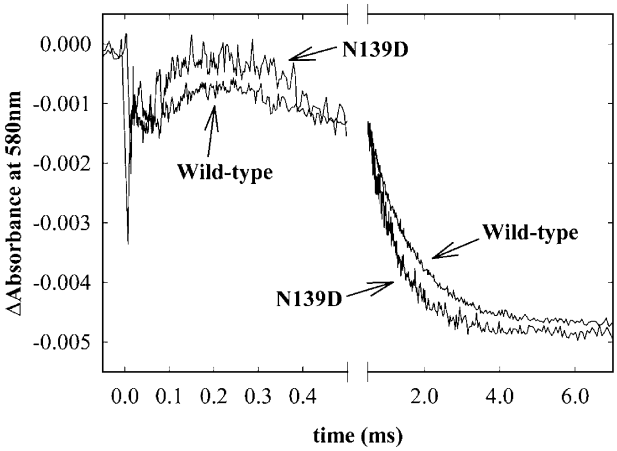

FIGURE 4: Absorbance changes at 580 nm as a function of time after flash photolysis of CO (at $t = 0$) from the fully reduced wild-type and N139D mutant enzymes in the presence of O_2, measured at 22 °C. The formation of intermediate **F** is seen as an absorbance increase in the time interval 50−200 μs. The subsequent decrease in absorbance is due to the decay of the **F** intermediate and formation of the fully oxidized enzyme. The data (measured at several different wavelengths) were fitted globally to a multiexponential function, and the rate of **F** formation was determined to be ~1×10^4 s^{-1} for both the wild-type and the mutant enzymes. The rate of **O** formation was ~2 times faster in the mutant enzyme (~1300 s^{-1}) compared to the wild-type enzyme (~700 s^{-1}). Experimental conditions: 0.1 M HEPES−KOH, pH 7.4, 0.1% dodecyl β-D-maltoside, ~1 μM reacting enzyme, and 1 mM O_2.

protons and the appearance of pumped protons outside the vesicles were measured by following absorbance changes in the pH indicator phenol red. The stopped-flow method has the advantage of a rapid response to pH changes and minimizes artifacts due to proton backflow into the vesicles. The data (Figure 2) are clear-cut and show no indication of proton pumping by the N139D mutant. In the presence of valinomycin, protons are clearly ejected (about 0.7 H^+/e^-) from the COVs prepared with the wild-type oxidase. When the proton ionophore FCCP is added to facilitate proton equilibration between the vesicle interior and exterior aqueous phases, there is a net alkalinization resulting from the chemical reaction ($4e^- + 4H^+ + O_2 \rightarrow 2H_2O$). The data with the N139D mutant show that there is no acidification (downward sweep of the curve in Figure 2) of the external solution accompanying the turnover of the enzyme.

Figure 3 shows the rereduction of the fully oxidized enzyme. In this experiment, the enzyme is prereduced by a mixture of dithionite and ruthenium hexaamine. Rapid mixing of this enzyme with a solution containing O_2 results in full oxidation of the enzyme, after which dithionite reacts to eliminate the excess O_2. This prepares the enzyme in the "pulsed" oxidized form, eliminating hysteretic effects that can result in artifacts due to the "resting" form of the enzyme (*47*). The freshly oxidized (pulsed) enzyme is then rereduced by the ruthenium(II) hexaamine in the solution, and the progress of the reaction is monitored optically with a diode array spectrophotometer. The time course of the reaction for the wild-type and N139D enzymes is shown in Figure 3. In each case, the experimental curve is fit to a two-exponential function. In both cases the fast phase accounts for most of the amplitude (~90%), with rates of 196 s^{-1} and 194 s^{-1} for the mutant and wild-type enzymes, respectively. It is concluded that the rate of reduction of the binuclear center is the same for the wild type and the N139D mutant and that the N139D mutation has no effect on the electron transfer from heme *a* to heme a_3 prior to the reaction with O_2.

In contrast, the reaction of the fully reduced enzyme with O_2 (Figure 4) shows that the N139D mutation results in significant acceleration of the last step (**F** → **O**) of the reaction sequence. This reaction was carried out using the flow-flash technique. The reaction was monitored at several wavelengths to observe changes in the redox states of heme *a* (605 nm), heme a_3 (580 nm; species **F**), and Cu_A (830 nm). Figure 4 shows the time course at 580 nm. The final downward phase reflects the electron transfer from heme *a* to the heme−copper center, resulting in the conversion of heme a_3 $Fe^{4+}{=}O^{2-}$ (oxoferryl species **F**) to the ferric heme a_3 (**O**xidized enzyme). This process is accelerated about 2-fold in the mutant enzyme (from 700 s^{-1} in the wild-type enzyme to 1300 s^{-1} in the N139D enzyme). The rate of formation of species **F** was the same in N139D as in the wild-type enzyme (1×10^4 s^{-1}). However, when species **F** is formed, the remaining electron in the Cu_A/heme *a* is distributed such that heme *a* is more reduced in the N139D mutant than in the wild-type oxidase. This suggests that the mutation results in an increase of the midpoint potential of heme *a*, at least in the **F** state of the enzyme.

The reaction of the fully reduced enzyme with O_2 was also examined at low temperatures [the so-called "slow-flash" technique (*41*)]. When the temperature is lowered to −24 °C, the rate of the reaction is slowed sufficiently so that a photodiode array can be used to acquire the full spectrum of the sample at different times during the reaction. This was done to determine if the spectra of the intermediates were altered by the mutation. The time course of the reaction, monitored at 580 nm, shows the formation and subsequent decay of species **F** (Figure 5). Whereas the rate of formation of **F** (**P** → **F** transition) appears similar to that of the wild type, the decay of species **F** (**F** → **O** transition) is about 2-fold faster with the N139D mutant. When the data surfaces

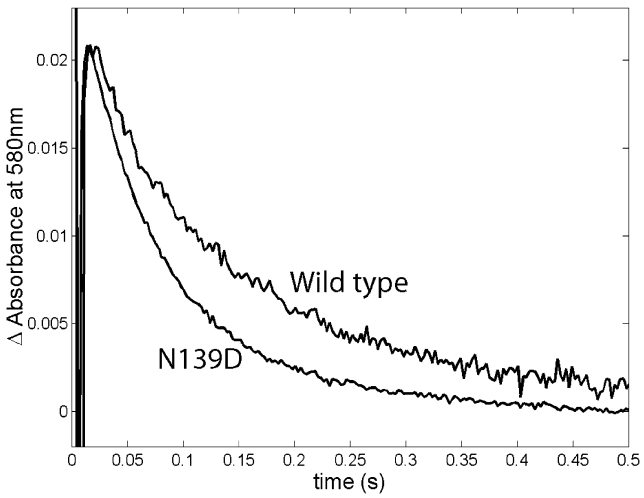

FIGURE 5: Low-temperature flow-flash kinetics. Time course data at 580 nm showing the formation and decay of the **F** intermediate in the wild-type and mutant enzymes at −24 °C. The rate of decay of the **F** intermediate of the mutant enzyme is about twice as fast as that of the wild-type enzyme, which agrees with the flow-flash data obtained at room temperature (Figure 4). Spectra of the intermediates, obtained by global fitting, are similar for the wild-type enzyme and the N139D mutant (not shown).

obtained from the wild-type and mutant oxidases were analyzed using the same global multiexponential algorithms [SPLMOD (*45*)], the component spectra were essentially the same. The detailed interpretation of the spectroscopic changes (not shown) will require further analysis, but the main point is that the components observed for both the wild type and mutant are essentially the same. It is concluded that the intermediates are not perturbed by the N139D mutation. The mutation has not altered the reaction mechanism of the oxygen chemistry at the active site.

DISCUSSION

The data presented show that the N139D mutation has unique characteristics that make it a potentially valuable tool to study the mechanism of the proton pump in cytochrome oxidase. The N139 residue is part of what appears in the structure of the oxidase to be a constriction in the proton-conducting D-channel, located just "above" the presumed entrance of the channel, D132 (see Figure 1). Replacing D132 by asparagine (D132N) effectively blocks the channel, consequently reducing enzyme turnover to less than 5% of the wild-type value (*30*, *33*, *34*). In single-turnover measurements, the consequences of the D132N mutation are most pronounced in the slow **F** → **O** conversion, i.e., the delivery of the last electron and proton to the heme−copper center during the catalytic cycle (*35*). In contrast, the N139D mutation results in substantially increased steady-state turnover (as much as 3-fold in some preparations) and an increased **F** → **O** transition rate, observed in the single-turnover reaction of the fully reduced enzyme with O_2. This in itself is a remarkable phenotype, but the interest in this mutation is particularly enhanced by the fact that the N139D mutant does not pump protons, as also reported for the corresponding mutant in the *P. denitrificans* oxidase (*25*). The oxidase activity of the *P. denitrificans* mutant is not reported to be higher than that of the wild type, but it is reported to be as active as the wild-type enzyme (*25*).

There is insufficient evidence to definitively explain the phenotype of the N139D mutant. Most other mutations in the D-channel have been reported to substantially decrease the oxidase activity and to decouple the residual activity from the proton pump (*30*, *48*−*51*). This report about the N139D mutant in *R. sphaeroides* is the first report of a mutant that increases the enzyme activity and still uncouples the proton pump from the redox function. The mutation exhibits considerable respiratory control, though less than the wild-type oxidase, which indicates that the mutant is still electrogenic and one or more rate-limiting steps are still involved in voltage generation. This is readily explained by the simple fact that the formation of water at the active site utilizes electrons and protons from opposite sides of the membrane. Hence, the mutation does not simply "uncouple" the enzyme by creating a transmembrane leak, since this would eliminate all respiratory control. It also demonstrates that protons are not taken up from the same side of the membrane as the electrons (P-side), which is what appears to occur in the D132N mutant of *R. sphaeroides* oxidase (*33*, *34*), which exhibits reverse respiratory control (i.e., oxidase activity decreases upon addition of uncouplers to reconstituted COVs).

It appears very likely that the D-channel provides protons, both for the chemistry at the active site and for the proton pump (*14*, *23*). This necessitates a gating switch (or switches) which prevents all of the protons from being consumed by the chemical reaction and which also prevents protons from slipping backward, thus maintaining net unidirectional flux through the pump mechanism. One can postulate a toggle switch which, in alternating positions, directs protons to either the oxygen reduction site (chemical protons) or to the exit channel (pumped protons). The N139D mutant acts as if this switch is held in a position so that the entire proton flux through the D-channel is directed to the active site. Since this toggle switch would no longer be directing half the protons to the exit channel, it is easy to rationalize why the oxidase activity would be enhanced.

This mechanical model, though useful, is, of course, both oversimplified and incomplete. The switch might correspond to a conformational change, in which case the explanation for the effect of N139D would be to lock the enzyme in a "chemical" vs a "pumping" conformational state. Since it is unlikely that the switch is located at N139, near the entrance of the D-channel, the effect of the mutation would need to be transmitted to a different location, such as to the vicinity of E286, which has been previously postulated to be at a branch point for proton flux (*52*, *53*), or to heme *a*. It is noted that the N139D mutation results in an apparent increase in the midpoint potential of heme *a*, at least in the **F** state of the enzyme. Hence, the mutation appears to have an influence on the electrostatic potential in the region of the protein near heme *a* and may be coupled to the pK_a values of groups in this part of the protein. The increased level of reduction of heme *a* could be related to the increased turnover rate in both the presence and absence of the membrane potential as well as to the elimination of proton pumping.

There are different but equally plausible explanations for the influence of the N139D mutation. Perhaps the essential feature of the N139D mutation is that it places an acidic residue within the D-channel. If this added aspartic acid has a high p*K*, it would be protonated in the oxidized enzyme

and, thus, would be able to provide a proton more rapidly than might otherwise be possible to a proton acceptor that is transiently generated during catalytic turnover. This might short circuit the proton pump by not allowing time for some critical changes to occur near the active site that are necessary to direct protons to the exit channel instead of to the partially reduced oxygen species. On the other hand, if the added aspartate were deprotonated (at least at some critical time during the catalytic cycle), D139 might draw protons away from a site in the exit channel and, by this mechanism, short circuit the pump mechanism.

Additional experiments may be able to distinguish these possibilities or suggest alternative explanations. The study of this and other mutations in the D-channel is likely to provide insight into critical mechanistic details of the proton pump of cytochrome oxidase.

ACKNOWLEDGMENT

J.M., A.S.P., and R.B.G. thank Ed Runyon of the University of Illinois Chemistry machine shop for machining the low-temperature cell holder; A.S.P. thanks Dr. Blanca Barquera for helping him to get started in mutagenesis.

REFERENCES

1. Garcia-Horsman, J. A., Barquera, B., Rumbley, J., Ma, J., and Gennis, R. B. (1994) *J. Bacteriol. 176*, 5587−5600.
2. Pereira, M. M., Santana, M., Soares, C. M., Mendes, J., Carita, J. N., Fernandes, A. S., Saraste, M., Carrondo, M. A., and Teixeira, M. (1999) *Biochim. Biophys. Acta 1413*, 1−13.
3. Pereira, M. M., Santana, M., and Teixeira, M. (2001) *Biochim. Biophys. Acta 1505*, 185−208.
4. Ferguson-Miller, S., and Babcock, G. T. (1996) *Chem. Rev. 7*, 2889−2907.
5. Soulimane, T., Buse, G., Bourenkov, G. P., Bartunik, H. D., Huber, R., and Than, M. E. (2000) *EMBO J. 19*, 1766−1776.
6. Ostermeier, C., Harrenga, A., Ermler, U., and Michel, H. (1997) *Proc. Natl. Acad. Sci. U.S.A. 94*, 10547−10553.
7. Abramson, J., Riistama, S., Larsson, G., Jasaitis, A., Svensson-Ek, M., Laakkonen, L., Puustinen, A., Iwata, S., and Wikström, M. (2000) *Nat. Struct. Biol. 7*, 910−917.
8. Iwata, S., Saynovits, M., Link, T. A., and Michel, H. (1996) *Structure 4*, 567−579.
9. Iwata, S., Ostermeier, C., Ludwig, B., and Michel, H. (1995) *Nature 376*, 660−669.
10. Tsukihara, T., Aoyama, H., Yamashita, E., Tomizaki, T., Yamaguchi, H., Shinzawa-Itoh, K., Nakashima, T., Yaono, R., and Yoshikawa, S. (1995) *Science 269*, 1069−1074.
11. Tsukihara, T., Aoyama, H., Yamashita, E., Takashi, T., Yamaguchi, H., Shinzawa-Itoh, K., Nakashima, R., Yaono, R., and Yoshikawa, S. (1996) *Science 272*, 1136−1144.
12. Yoshikawa, S., Shinzawa-Itoh, K., Nakashima, R., Yaono, R., Yamashita, E., Inoue, N., Yao, M., Fei, M. J., Libeu, C. P., Mizushima, T., Yamaguchi, H., Tomizaki, T., and Tsukihara, T. (1998) *Science 280*, 1723−1729.
13. Yoshikawa, S., Shinzawa-Itoh, K., and Tsukihara, T. (2000) *J. Inorg. Biochem. 82*, 1−7.
14. Michel, H. (1999) *Biochemistry 38*, 15129−15140.
15. Wikström, M. (2000) *Biochemistry 39*, 3515−3519.
16. Zaslavsky, D., and Gennis, R. B. (2000) *Biochim. Biophys. Acta 1458*, 164−179.
17. Verkhovsky, M. I., Jasaitis, A., Verkhovskaya, M. L., Morgan, J. E., and Wikström, M. (1999) *Nature 400*, 480−483.
18. Ruitenberg, M., Kannt, A., Bamberg, E., Fendler, K., and Michel, H. (2002) *Nature 417*, 99−102.
19. Pecoraro, C., Gennis, R. B., Vygodina, T. V., and Konstantinov, A. A. (2001) *Biochemistry 40*, 9695−9708.
20. Brändén, M., Sigurdson, H., Namslauer, A., Gennis, R. B., Ädelroth, P., and Brzezinski, P. (2001) *Proc. Natl. Acad. Sci. U.S.A. 98*, 5013−5018.
21. Ädelroth, P., Gennis, R. B., and Brzezinski, P. (1998) *Biochemistry 37*, 2470−2476.
22. Gennis, R. B. (1998) *Biochim. Biophys. Acta 1365*, 241−248.
23. Konstantinov, A. A., Siletsky, S., Mitchell, D., Kaulen, A., and Gennis, R. B. (1997) *Proc. Natl. Acad. Sci. U.S.A. 94*, 9085−9090.
24. Wikström, M., Jasaitis, A., Backgren, C., Puustinen, A., and Verkhovsky, M. I. (2000) *Biochim. Biophys. Acta 1459*, 514−520.
25. Pfitzner, U., Hoffmeier, K., Harrenga, A., Kannt, A., Michel, H., Bamberg, E., Richter, O.-M. H., and Ludwig, B. (2000) *Biochemistry 39*, 6756−6762.
26. Cappuccio, J. A., Ayala, I., Elliott, G. I., Szundi, I., Lewis, J., Konopelski, J. P., Barry, B. A., and Einarsdóttir, Ó. (2002) *J. Am. Chem. Soc. 124*, 1750−1760.
27. McCauley, K. M., Vrtis, J. M., Dupont, J., and van der Donk, W. A. (2000) *J. Am. Chem. Soc. 122*, 2403−2404.
28. Proshlyakov, D. A., Pressler, M. A., DeMaso, C., Leykam, J. F., DeWitt, D. L., and Babcock, G. T. (2000) *Science 290*, 1588−1591.
29. Blomberg, M. R. A., Siegbahn, P. E. M., Babcock, G. T., and Wikström, M. (2000) *J. Inorg. Biochem. 80*, 261−269.
30. Fetter, J. R., Qian, J., Shapleigh, J., Thomas, J. W., Garcia-Horsman, A., Schmidt, E., Hosler, J., Babcock, G. T., Gennis, R. B., and Ferguson-Miller, S. (1995) *Proc. Natl. Acad. Sci. U.S.A. 92*, 1604−1608.
31. Zaslavsky, D., and Gennis, R. B. (1998) *Biochemistry 37*, 3062−3067.
32. Vygodina, T. V., Pecoraro, C., Mitchell, D., Gennis, R., and Konstantinov, A. A. (1998) *Biochemistry 37*, 3053−3061.
33. Mills, D. A., Florens, L., Hiser, C., Qian, J., and Ferguson-Miller, S. (2000) *Biochim. Biophys. Acta 1458*, 180−187.
34. Fetter, J., Sharpe, M., Qian, J., Mills, D., Ferguson-Miller, S., and Nicholls, P. (1996) *FEBS Lett. 393*, 155−160.
35. Ädelroth, P., Ek, M. S., Mitchell, D. M., Gennis, R. B., and Brzezinski, P. (1997) *Biochemistry 36*, 13824−13829.
36. Aagaard, A., Gilderson, G., Mills, D. A., Ferguson-Miller, S., and Brzezinski, P. (2000) *Biochemistry 39*, 15847−15850.
37. Backgren, C., Hummer, G., Wikström, M., and Puustinen, A. (2000) *Biochemistry 39*, 7863−7867.
38. Puustinen, A., and Wikström, M. (1999) *Proc. Natl. Acad. Sci. U.S.A. 96*, 35−37.
39. Garcia-Horsman, J. A., Puustinen, A., Gennis, R. B., and Wikström, M. (1995) *Biochemistry 34*, 4428−4433.
40. Mitchell, D. M., and Gennis, R. B. (1995) *FEBS Lett. 368*, 148−150.
41. Morgan, J. E., Verkhovsky, M. I., and Wikström, M. (1996) *Biochemistry 35*, 12235−12240.
42. Verkhovsky, M. I., Morgan, J. E., and Wikström, M. (1995) *Biochemistry 34*, 7483−7491.
43. Hosler, J. P., Fetter, J., Tecklenberg, M. M. J., Espe, M., Lerma, C., and Ferguson-Miller, S. (1992) *J. Biol. Chem. 267*, 24264−24272.
44. Hiser, C., Mills, D. A., Schall, M., and Ferguson-Miller, S. (2001) *Biochemistry 40*, 1606−1615.
45. Provincer, S. W., and Vogel, R. H. (1983) *Prog. Sci. Comput. 2*, 304−319.
46. Morgan, J. E., Verkhovsky, M. I., Puustinen, A., and Wikström, M. (1995) *Biochemistry 34*, 15633−15637.
47. Antonini, E., Brunori, M., Colosimo, A., Greenwood, C., and Wilson, M. T. (1977) *Proc. Natl. Acad. Sci. U.S.A. 74*, 3128−3132.
48. Pfitzner, U., Odenwald, A., Ostermann, T., Weingard, L., Ludwig, B., and Richter, O.-M. H. (1998) *J. Biomembr. Bioenerg. 30*, 89−93.
49. Garcia-Horsman, J. A., Puustinen, A., Gennis, R. B., and Wikström, M. (1995) *Biochemistry 34*, 4428−4433.
50. Thomas, J. W., Puustinen, A., Alben, J. O., Gennis, R. B., and Wikström, M. (1993) *Biochemistry 32*, 10923−10928.
51. Verkhovskaya, M. L., Garcia-Horsman, A., Puustinen, A., Rigaud, J.-L., Morgan, J. E., Verkhovsky, M. I., and Wikström, M. (1997) *Proc. Natl. Acad. Sci. U.S.A. 94*, 10128−10131.
52. Hofacker, I., and Schulten, K. (1998) *Proteins 30*, 100−107.
53. Pomes, R., Hummer, G., and Wikström, M. (1998) *Biochim. Biophys. Acta 1365*, 255−260.
54. Humphrey, W., Dalke, A., and Schulten, K. (1996) *J. Mol. Graphics 14*, 33−38.

BI026582+